Proceedings of the ASME 2014 International Mechanical Engineering Congress & Exposition
IMECE2014
November 14-20, 2014, Montreal, Quebec, Canada

IMECE2014-40269

USING INFRARED THERMOGRAPHY AND BIOSENSORS TO DETECT THERMAL DISCOMFORT IN A BUILDING'S INHABITANTS

Mihai Burzo*
Mechanical Engineering
University of Michigan-Flint
Flint, MI 48502, USA
mburzo@umich.edu

Mohamed Abouelenien
Computer Science and Engineering
University of Michigan
Ann Arbor, MI 48109, USA
zmohamed@umich.edu

Verónica Pérez-Rosas
Computer Science Engineering
University of North Texas
Denton, TX 76207, USA
veronicaperezrosas@my.unt.edu

Cakra Wicaksono
Mechanical and Energy Engineering
University of North Texas
Denton, TX 76207, USA
CakraWicaksono@my.unt.edu

Yong Tao
Mechanical and Energy Engineering
University of North Texas
Denton, TX 76207, USA
Yong.Tao@unt.edu

Rada Mihalcea
Computer Science and Engineering
University of Michigan
Ann Arbor, MI 48109, USA
mihalcea@umich.edu

ABSTRACT

This paper lays the grounds for a new methodology for detecting thermal discomfort, which can potentially reduce the building energy usage while improving the comfort of its inhabitants. The paper describes our explorations in automatic human discomfort prediction using physiological signals directly collected from a buildings inhabitants. Using infrared thermography, as well as several other bio-sensors (galvanic skin response, heart rate tracker, respiration rate tracker), we record a building's inhabitants under various thermal conditions (hot, cold, neutral), and consequently build a multimodal model that can automatically detect thermal discomfort.

The paper makes two important contributions. First, we introduce a novel dataset, consisting of sensorial measurements of human behavior under varied comfort/discomfort conditions. The change in physiological signals of the human body are monitored for several subjects, for different comfort levels in an indoor environment. Second, using the dataset obtained in the first step, we build a model that identifies the relationship between human factors, as tracked through infrared thermography and other bio-sensors, and environmental conditions related to discomfort. Third, we measure the correlation between sensorial measurements collected from the user and self-reported levels of discomfort, and hence identify the sensorial measurements that are predictive of human discomfort. The final goal is to automatically predict the level of discomfort of a building inhabitant without any explicit input from the user.

This human-centered discomfort prediction model is expected to enable innovative adaptive control scenarios for a built environment conditions in real time, as well as a significant reduction in building energy usage directly related to human occupancy and their desired comfort levels.

INTRODUCTION

Recent statistics indicate that over 41% of the U.S. primary energy is consumed by the buildings sector [1], with resident buildings accounting for 54% of this energy consumption, and the remaining 46% for commercial buildings. Effective energy management in the buildings is one of the key factors impacting the overall energy consumption, and thus has important consequences on climate and the environment. The increased energy consumption is related for the most part to the process of achieving thermal comfort by the buildings' occupants. This increase

*Address all correspondence to this author.

contributes directly to the problem of global warming and is predicted to increase along with carbon dioxide emissions in the next years [2, 3].

The trade-off between achieving thermal comfort and reducing energy consumption encouraged the construction of energy-efficient buildings. Construction of these buildings aims at controlling the thermal conditions in order to ensure a proper thermal comfort level for their occupants while minimizing heat loss. Otherwise, occupants can seek other means to restore comfort, such as adjustment of furnaces, air conditioners and fans or adding space heaters, which will further increase energy consumption. The reduction in energy consumption would have useful consequences on the climate and the environment. Human behavior studies have shown that individuals spend more than 90 % of their time indoors as compared to 10% of their time outdoors during the summer, and 4% during the winter [4]. Hence, early detection of thermal discomfort and automatic restoration of thermal comfort can potentially lead to significant reduction in the energy consumption of buildings.

Effective energy management strategies can be used to design energy-efficient buildings and furthermore impact the overall energy consumption. Following this line of research, this paper proposes a new methodology for detecting thermal discomfort, which can potentially reduce the building energy usage while improving the comfort of its inhabitants. In particular, we focus on automatically detecting human discomfort using thermal features obtained from an infrared thermal camera and collected from a building's occupants.

The paper contributes a novel dataset consisting of sensorial measurements of the human body and a multimodal model that automatically detects thermal discomfort based on thermal measurements physiological measurements obtained from the occupants. The data was collected using a thermal camera that records thermal videos of the face area of the subject, and several bio-sensors including galvanic skin response, heart rate tracker, and respiration rate tracker. These measurements were collected from the occupants at different levels of comfort. In addition to the collected data, self-reported levels of discomfort were obtained using the Predicted Mean Vote (PMV) model.

To identify the relationship between the measurements obtained and thermal discomfort of the occupants, we introduce a multimodal system that automatically predicts the level of discomfort of the building's occupants without any explicit action from the user. The system relies mainly on the thermal features obtained from the thermal camera owing to its advantage as a noninvasive and noncontact method. Moreover, the collected physiological measurements are first compared to the results obtained by the existing system and then integrated into the system to observe whether or not it enhances the system. A possible application for this system is to maintain the thermal comfort of building occupants without any manual actions from the occupant, while keeping the environmental parameters at the value that yields minimum building energy consumption.

RELATED WORK

Thermal comfort can be defined from psychological, thermo-physiological, and heat-balance perspectives [5]. According to the psychological definition, thermal comfort is "That condition of mind which expresses satisfaction with the thermal environment" [6]. From the thermo-physiological perspective, thermal comfort is the minimum rate of nervous signals from the thermal receptors in the skin [7]. According to the heat-balance definition, thermal comfort is reached when the heat flow from and to the skin due to metabolism is balanced [8].

Measuring thermal comfort is challenging due to the subjective assessment and the psychological aspects [9, 10]. Additionally, the rate of metabolism differs from one individual to the other. The ASHRAE 55- standard defines metabolic rate as the rate of transformation of chemical energy into thermal energy and mechanical work due to metabolic activities.

In general, there are six main factors that indicate thermal comfort. They can be divided into personal and environmental factors. Personal factors include metabolic rate and clothing insulation. In this paper, we limit the effect of personal factors by controlling the activity rate and clothing. The environmental factors include air temperature, mean radiant temperature, air velocity, and relative humidity. Air temperature is measured from the immediate surrounding environment of the occupants. Mean radiant temperature expresses the effect of the temperature of the surrounding objects on the thermal comfort of the occupants [11]. Air velocity describes the rate of air movement across the occupant and has an important contribution to the (convective) heat transfer from the body. Relative humidity is the ratio between the actual water vapor present in the air to the maximum amount of water vapor needed for saturation at a given temperature.

Thermal imaging is a non-contact non-invasive mean to capture thermal measurements from heat-emitting sources with many applications in a variety of fields such as the military and medical fields [12–14]. It was recently used as a mean to detect discomfort of human owing to its advantage as a contact free method. Based on a study on infrared thermography in humans [15], Oliveira et al. [16] used infrared thermal imaging to extract thermal regions of interest from the faces and applied fast Fourier transform to analyze these regions to assess thermal discomfort. Oliveira and Moreau [17] assessed the thermal sensation using different airflow temperatures and airflow fluctuations. They conducted their experiments using thermal imaging and concluded that airflow temperature influenced the sensation of thermal discomfort. Zeiler et al. [18] analyzed the critical indicators of the human sensation of comfort in mild cool office environments by including the human body as a sensor using infrared imaging. Maia et al. [19] proposed a decision-tree model to evaluate the thermal comfort of horses using infrared thermography imaging.

Experiments have been conducted to analyze the thermal comfort of individuals considering both environmental and personal factors in indoor environments. Freire et al. [20] introduced two control algorithms, one to achieve thermal comfort optimization while the other to achieve energy consumption minimization while maintaining the indoor thermal comfort using only-one-actuator system. Haldi and Robinson [21] applied probabilistic modeling using logistic regression to study the action of occupants sensing thermal discomfort in an indoor environment. Huizenga et al. [22] surveyed over 30,000 occupants in 215 buildings and concluded that high rates of thermal discomfort occurred in most buildings. Fang et al. [23] analyzed the effect of air temperature, humidity, and ventilation on the thermal comfort of office workers. Zheng et al. [24] studied the relation between thermal comfort and the air quality and ventilation in indoor office buildings. Balaras et al. [25] investigated hospital operation rooms in order to achieve energy conservation without sacrificing the thermal comfort and the quality of services provided for patients. Ye et al. [26] investigated the thermal sensation of occupants in naturally ventilated buildings, where they applied an adaptive comfort model. Bessoudo [27] studied the impact of climate, glazing type, and shading properties on thermal comfort in an office environment in order to design energy-efficient buildings. Homod et al. [28] used PMV/PPD to detect thermal discomfort and combined a fuzzy model with a Gauss-Newton method for nonlinear regression algorithm in order to effectively control indoor thermal comfort. Hamdy et al. [29] studied the energy usage as well as the size of the cooling equipment required to achieve thermal comfort in an office building.

The effect of thermal comfort on individuals in an outdoor environment was evaluated for applications such as pedestrian comfort. Stathopoulos et al. [30] analyzed the integrated effect of air temperature, air velocity, relative humidity, and solar radiation on the human thermal comfort in an urban environment. Zhang and He [31] suggested strategies such as usage of solar shading in order to improve the thermal sensation of pedestrians in streets. Toudert and Mayer [32] conducted thermal experiments to show the effect of shading and surrounding surfaces on reducing thermal stress on individuals in an outdoor environment.

Multiple measurements are often taken to be able to accurately determine the main contributors to the sensation of discomfort. Ismail et al. [33] used thermal comfort multi-station to measure air temperature, air speed, relative humidity, illumination, and metabolism of students in a lab and determined that humidity and indoor air speed have the largest effect on sensing discomfort.

Physiological measurements can be also used to analyze the human body in order to determine how it is affected by thermal discomfort. It has been shown that temperature and skin conductance are important indicators of human thermal response [34]. Other measurements such as blood flow plays also a critical role in heat transfer between the body core and the skin. In cold weather, vasoconstriction occurs, which results in narrowing the blood vessels in the body to decrease the blood flow and keep the heat. On the other hand, in hot weather, vasodilation occurs, which results in increasing the width of the blood vessels. Accordingly, adapting thermally to hot weather is faster than cold weather [5]. Overall it turns out that physiological measurements are fundamental in detecting thermal discomfort.

FIGURE 1. ZERO ENERGY BUILDING, WHERE THE EXPERIMENTS TOOK PLACE.

Multimodal environmental sensors have been recently used to detect discomfort. Dang et al. [35, 36] constructed pedestrian navigation systems that choose passes to reduce thermal discomfort for pedestrians. The research organized the massive data generated by the sensors using a multi-factor cost model and a data fuser in order to integrate multimodal data together in terms of thermal discomfort cost.

EXPERIMENTAL SETUP

Measurement Apparatus and Data Collection

Experiments were conducted in an area which was set-up as a typical living room in the Zero Energy Laboratory shown in Fig. 1, located at the University of North Texas (UNT). Fourteen (14) graduate students from the College of Engineering participated in the experiments. The sample consisted of 3 female and 11 male participants with ages ranging between 22 and 35 years.

Thermal and visual videos, in addition to physiological and environmental measurements, were collected for all participants as described in the next few paragraphs. An overview of the measurement system and procedure is presented in the diagram shown in Fig. 2.

The thermal videos were recorded using a Flir Thermovision A40 thermal camera at a rate of 60 frames per second. Sample thermal frames can be seen in Fig. 3, where different ranges of colors indicate different temperatures (higher temperatures are represented by lighter colors). The feature extraction process from the thermal videos is described below. Visual videos of the occupants were also recorded simultaneously with the thermal videos.

Physiological measurements were collected using four type

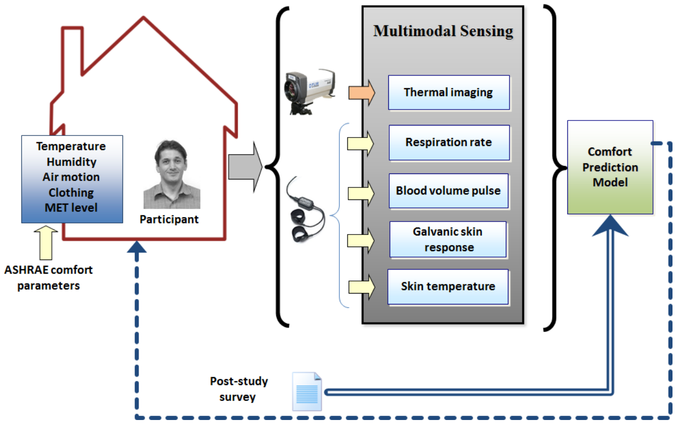

FIGURE 2. AN OVERALL VIEW OF OUR MULTIMODAL SYSTEM, WHICH INCLUDES THE COLLECTION OF THERMAL IMAGING OF FACIAL FEATURES AND PHYSIOLOGICAL AND ENVIRONMENTAL MEASUREMENTS IN ADDITION TO A THERMAL SENSATION SURVEY.

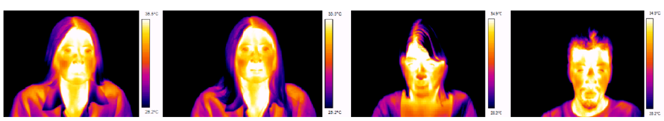

FIGURE 3. EXAMPLES OF THERMAL FRAMES.

of Thought Technology's FlexComp Infiniti sensors, shown in Fig. 4, that were attached to the non-dominant hand of the participants. Two skin conductance electrodes were placed on the second and third fingers whereas the skin temperature and blood volume pulse sensors were placed at the thumb and index fingers respectively. A respiration rate sensor (belt over chest design) was also used. Measurements included: blood volume pressure (BVP), skin temperature (ST), respiration rate (R), and skin conductance (SC). The output of each sensor was obtained from a multimodal encoder connected to the main computer using an USB interface device. We recorded the combined output with the Biograph Infinity Physiology suite software, which allowed us to visualize and control the data acquisition process. We decided to take all the physiological measurements at a rate of 2048/sec, which was the maximum rate allowed by the device, in order to collect as much raw data as possible for accurate processing.

Environmental measurements were collected using HOBO Data Loggers sensors and included the building's air temperature and relative humidity. The wall temperature was also recorded using Newport True RMS super meter and the air speed inside the room was measured using an Omega HHF1000 sensor according to ASHRAE standard 55. The air and wall temperatures were recorded to make sure that they are in a fixed range of 73°F to 76°F during the experiments. This range was preset in order to have a controlled environment in the room to avoid external

FIGURE 4. PHYSIOLOGICAL SENSORS.

temperature effect on the participants and devices. Moreover, we wanted the default room temperature to be in a comfortable range to the participants as recommended by the WestMidlands Public Health Observatory.

Relative humidity was in the percentage range of lower to higher 50s. An electric fan was used in one stage of the experiments as explained below. The air speed was in the range of $0.8m/s$ to $3m/s$ for all the subjects. Additionally, clothing for all the subjects was limited to 0.57 Clo and the metabolic rate was controlled by specific metabolic activities. These settings were designed to eliminate external factors on the process of detecting discomfort.

Three-Stage Comfort Conditions

For each subject the experiment was divided into three stages, which required a total time of 30 minutes for each one of the 14 subjects (building's occupants). In the first stage, the individuals performed a 10 minutes workout on an air resistance elliptical machine inside the Zero Energy building. A metronome was provided to make sure that the exercise technique of all the human subjects was uniform, such that approximately 2.8 metabolic rate was performed by each subject during this activity. The activity was designed to produce an increase in the heat level of the human body and to observe its effect on thermal comfort level. After the activity, each occupant is asked to immediately sit on a chair where the four physiological measurements, in addition to the thermal and visual videos, were recorded for five minutes. Note however that the first recorded 10 seconds were used for our analysis.

In the second stage, the same measurements and recordings were collected for four additional minutes following the end of stage one. For this stage, 10 seconds of the four minutes were used for data analysis. This stage simulates the adaptation of the human body to the surroundings and the relaxation back to a condition of no effort or activity and therefore a condition of comfort.

In the third stage, an electric fan creates an air flow in front of each occupant for a period of 10 minutes. The physiological measurements and video recordings were collected for two minutes close to the end of the 10 minutes period, however, 10 seconds were used for our analysis. This stage identifies the effect of air movement across the occupant's body after relaxation with no activity and determines its effect on the thermal discomfort level. The continued airflow targets a constant cooling discomfort sensation by the occupants. The intent for the above described three stages was to effectively create a perceived sensation of "hot" discomfort, comfort and "cold" discomfort.

Overall, the collection consists of 42 thermal videos, 42 visual videos, and 42 sets of physiological measurements, where each set has four types of physiological measurements. To eliminate transition periods between discomfort and comfort states, we experimented with two time frames for each stage: we used 10 and 120 seconds per stage with thermal video recordings of 150 and 1800 frames, respectively. Both time periods achieved close performance, but due to space limitations, we only report here the results obtained with the 10 seconds period. We refer to these experiments as the $stage-wise experiments$, where each occupant has three videos labeled according to the simulated experimental stages as hot discomfort, comfort, and cold discomfort. This setting results in an equal distribution of 14 instances per class.

Comfort Level Survey

In order to also evaluate the *experienced* comfort level, we use the Predicted Mean Vote/Predicted Percentage of Dissatisfied or PMV/PPD model developed by Fanger [8,37], which assumes steady state conditions in an indoor environment. The PMV rates thermal sensation of the subjects on a scale of (-3) for cold to (3) for hot. The surveyed individuals choose a value on the thermal scale to express their thermal sensation. PPD can be determined from PMV following that PPD increases when PMV shifts away in both directions from neutral, which is represented as (0) on the thermal scale.

We controlled the clothing and metabolic rate as described in the section above. Participants were surveyed one time for each of the three stages of the experiments on their thermal comfort sensation following the PMV scale. The scale has seven divisions that range from (3) for hot in decrements of one down to (-3) for cold. The first survey was taken right after the 10 minutes period of activity during the first stage. The second survey was conducted after the end of the four minutes period of the second (cooling down) stage. The third survey was conducted at the end of the third stage, after the fan operated for 10 minutes. The answers to the survey questions were collected in order to investigate the relationship between the reported levels of thermal comfort/discomfort and the extracted features in order to automatically detect discomfort. This setting provided a different distribution of class labels among the occupants. In particular, 18, 9, and 15 videos were labeled as hot discomfort, comfort, and cold discomfort, respectively. We refer to these experiments as the PMV-labeled experiments.

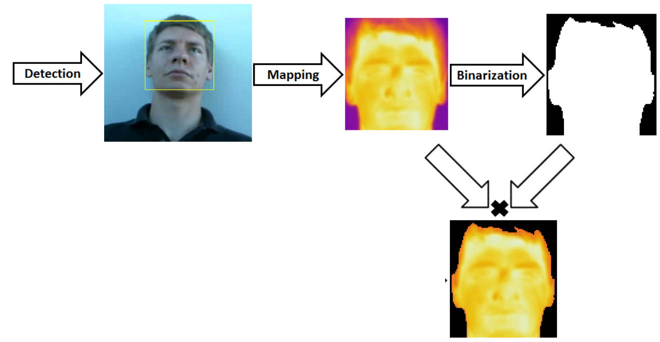

FIGURE 5. AN OVERVIEW OF THE PROCESS OF AUTOMATIC DETECTION OF THERMAL FACES.

METHODOLOGY

Face Detection and Mapping

The first step to pre-process our thermal videos in order to extract meaningful features is to detect the face areas of the occupants. The face detection process was not very successful when applied directly on the thermal images due to the absence of clear edges and the lower resolution of the thermal images compared to the visual ones. Given that the visual and thermal videos were recorded simultaneously with fixed optics (i.e., the distance between thermal and visual camera objectives and the subject was constant), we detected the faces from the visual frames using the Viola-Jones algorithm [38] and then we mapped it automatically to the thermal frames. The algorithm uses the sum of the images pixel values within multiple rectangular areas to detect the faces. The mapping required the knowledge of the pixel-wise distance between the visual and thermal optics and then was applied automatically to all thermal images.

Despite the accurate thermal face detection process, the corners of the detected faces might contain parts of the background. Additionally, large areas of hair might also add noise. To handle this problem and eliminate the effect of these parts, we cropped the face detected areas from the images and converted them to binary images with two pixel values, (1) for white and (0) for black. The face areas are represented by the white pixels while other parts are transformed to black. The image binarization process thresholds the values of the original image pixels using Otsu's method [39] depending on the pixels intensities in order to reduce the intra class variance between the white and black pixels. Hence, the detected face images (before binarization) is multiplied by the binary image to eliminate the background and noisy pixels while keeping the non-zero pixels. An overview of the detection of thermal faces can be seen in Fig. 5.

Feature Extraction and Classification

In order to automatically identify the level of comfort of the building's occupants, we propose two feature extraction approaches, namely, bag of visual words and feature selection. Both approaches were applied to both the stage-wise and the PMV-labeled experiments.

In general, the bag of visual words method has three stages, point detection, feature description, and codebook generation. Given some videos, the point detection phase searches for interesting points in each video frame, such as edges. These points are then described using feature descriptors to create feature vectors in order to represent each frame. The vectors are then clustered, where the centers of the clusters are referred to as codewords or visual words. These codewords form our codebook. The final output is the frequency of occurrence of the feature vectors of each video in the clusters, such that each video is represented by one vector that has a size equal to the number of clusters.

For our experiments, we use all non-zero pixels as the detected points of interest, a histogram of the values of the pixels for feature description, and k-means clustering for codebook generation. First, the non-zero pixels of the thermal face images (i.e., the output of Fig. 5) for all three stages are detected. Second, the pixel values of the images create a histogram with 256 bins for each image (an image pixel values range from 0 to 255). However, given that the count of black pixels of zero value was discarded, we have a vector of size 255 to describe each image. Analyzing 10 seconds per video recording generates a total of 6300 vectors. Finally, the histogram vectors are used to generate clusters using k-means clustering, where the cluster centers are the codewords. Each cluster contains similar or closely related vectors. Following this, a single vector is created for each video that has the same size as the number of clusters. The values in this final vector correspond to the occurrence count of the histogram vectors in each cluster, i.e., frequency of occurrence of the features of each video in each cluster. Given any test video, histogram vectors are generated from its frames and are matched to the nearest codewords to form a single test vector formed of the occurrence count over its codewords vocabulary.

Using the second approach, four features are extracted from the thermal videos. The values of the image pixels represent different colors. Lighter colors have higher pixel values which correspond to higher temperatures. For the detected face areas, the four extracted features are the average value of all non-zero pixels, the maximum pixel value, the minimum pixel value, and the difference between the maximum and minimum pixel values. These four features are additionally averaged over all the frames belonging to each video, which results in a feature vector of size four to represent each video.

We conducted our experiments using Plus-L Take-Away-R feature selection method [40] to detect the best feature or combination of features that achieves the highest performance. The method is a sequential search strategy that moves forward by adding L features and backward by removing R features in search for the best combination of features. In our experiments, we use $L = 1$ and $R = 2$: starting with a set of four thermal features, we remove two features and then add one and so on. This feature selection method is applied to the four thermal features, the four physiological features, and the eight features combined.

The last step is training classifiers to create a model that is able to classify unseen data into their proper classes as an indicator of hot discomfort, comfort, or cold discomfort. The classification processes uses leave-one-out cross validation. For instance in our case, each video is used 41 times for training and one time for testing. For both feature extraction approaches, three classifiers are trained, decision tree, K-nearest neighbor (K=3), and Naive Bayes classifiers. The overall average performance over the cross validations is reported along with the average per class accuracy.

EXPERIMENTAL RESULTS

To evaluate the performance of our experiments, the overall accuracy was measured in addition to the per class accuracy. This will give an idea of the capability of our approaches of detecting thermal discomfort/comfort. The baseline performance is calculated according to the random guessing accuracy. The stage-wise experiments have equally distributed instances among the three classes, which allowed a random guessing accuracy of approximately 33.3% per class. The PMV-labeled experiments have 18, 9, and 15 instances labeled as hot discomfort, comfort, and cold discomfort, respectively, which resulted in a random guessing accuracy of approximately 42.9%, 21.4%, and 35.7%, respectively.

Bag of Visual Words Approach

Following our bag of visual words approach, the only variable that can be manipulated is the number of clusters. We decided to use 5, 15, and 30 clusters to observe whether increasing the number of our codewords can further improve the results.

Figure 6 (A), (B), and (C) show the accuracy of the bag of visual words approach with decision trees, nearest neighbor, and Naive Bayes, respectively, for the stage-wise experiments using 5, 15, and 30 clusters. The overall accuracy lies between 60 to 70%. The per class accuracy is close for all three classes using decision trees and Naive Bayes. Using nearest neighbor, the hot discomfort class achieves above 90% classification accuracy using 5 clusters. However, this improvement is on the expense of the other two classes and, in particular, the comfort class. It can also be noted that as we increase the number of clusters, the performance is deteriorated for all classifiers.

Figure 6 (D), (E), and (F) show the accuracy for the PMV-labeled experiments. Clearly, using the self-reported level of discomfort using the PMV scale results in lower overall accuracy compared to the stage-wise experiments. Although there is improvement for detecting the hot discomfort class, this improvement is also on the expense of the other classes. For example, using Naive Bayes classifier, the comfort class is never classified correctly for any number of clusters.

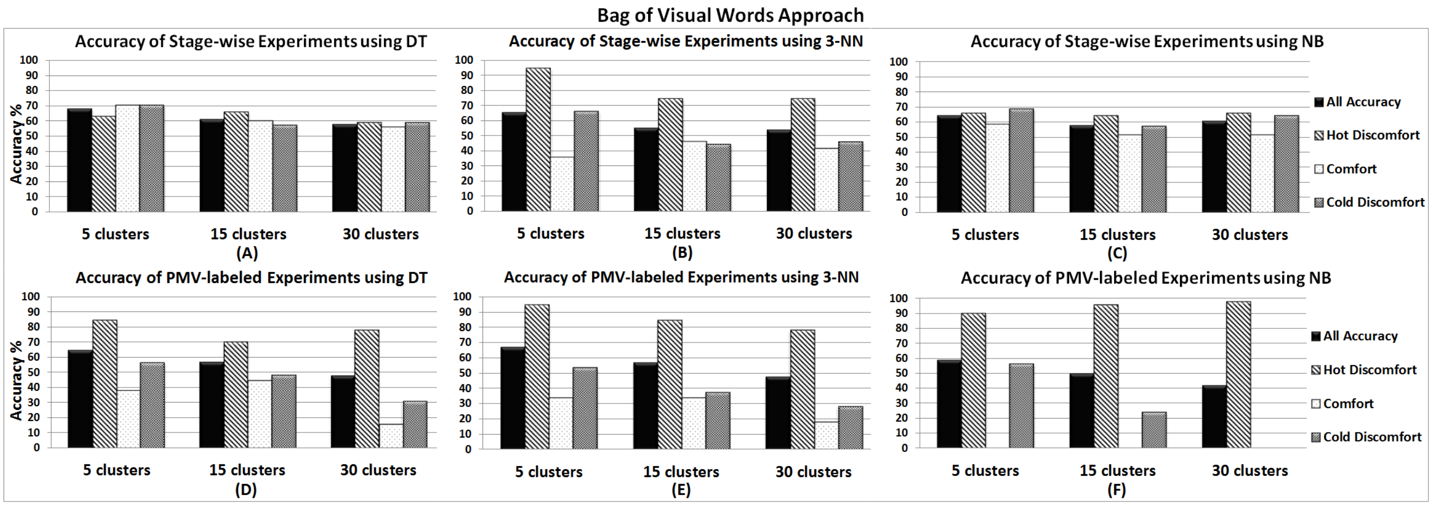

FIGURE 6. BAG OF VISUAL WORDS OVERALL AND PER CLASS ACCURACY PERCENTAGES FOR STAGE-WISE EXPERIMENTS USING (A) DECISION TREES (DT), (B) K-NEAREST NEIGHBOR (3-NN), AND (C) NAIVE BAYES (NB), AND FOR PMV-LABELED EXPERIMENTS USING (D) DECISION TREES (DT), (E) K-NEAREST NEIGHBOR (3-NN), AND (F) NAIVE BAYES (NB).

Feature Selection Approach

Using the feature selection approach, we start by reporting the accuracy of training all four thermal features, all four physiological features, and all eight features combined. We then report the performance of individual features to indicate which features are highly discriminative between the levels of discomfort. We additionally report the accuracy of the selected features which achieve the best performance in indicating the level of discomfort using the Plus-L Take-Away-R method for the thermal features, physiological features, and all eight features.

Figure 7 displays the accuracy percentages without eliminating any of the features. It can be clearly noticed that training the thermal features achieves improved performance compared to training the physiological features using all classifiers. For instance, an improvement of 93% is observed using decision trees in Fig 7 (A) in the overall accuracy. The only exception can be seen for the PMV-labeled experiments in Fig. 7 (F), where the physiological features achieve a slight improvement over the thermal features in the overall accuracy. In several cases, the performance does not reach that of the baseline such as the performance of the comfort and cold comfort classes in Fig. 7 (B) using nearest neighbor. Training all physiological and thermal features combined does not add to the performance of relying solely on the thermal features, except for a slight increase in accuracy using a Naive Bayes classifier for both the stage-wise and PMV-labeled experiments.

As with the bag of words results, the overall accuracy of the stage-wise experiments is better than that of the PMV-labeled. Moreover, the comfort class also suffers a deteriorated performance while the hot discomfort class performance is improved in the PMV-labeled experiments.

TABLE 1. AVERAGE OVERALL ACCURACY % (ALL) AND AVERAGE PER CLASS ACCURACY % FOR HOT DISCOMFORT (HOT), COMFORT (COMF), AND COLD DISCOMFORT (COLD) FOR EACH FEATURE USING DECISION TREES. THE BEST PERFORMANCE IS HIGHLIGHTED IN BOLD. THE FEATURES INCLUDE: THERMAL PIXELS AVERAGE (AVG), MAXIMUM PIXEL VALUE (MAX), MINIMUM PIXEL VALUE (MIN), DIFFERENCE BETWEEN MAXIMUM AND MINIMUM (MAX/MIN), BLOOD VOLUME PRESSURE (BVP), SKIN TEMPERATURE (ST), RESPIRATION RATE (R), AND SKIN CONDUCTANCE (SC).

	Stage-wise				PMV-labeled			
Feat\Acc.	ALL	HOT	COMF	COLD	ALL	HOT	COMF	COLD
avg	**76.2**	57.1	**78.6**	**92.9**	47.6	50.0	22.2	60.0
max	52.4	50.0	42.9	64.3	50.0	61.1	22.2	53.3
min	52.4	42.9	35.7	78.6	**52.4**	**66.7**	0.0	**66.7**
max/min	45.2	35.7	35.7	64.3	42.9	**66.7**	11.1	33.3
BVP	59.5	**64.3**	71.4	42.9	35.7	61.1	0.0	26.7
ST	40.5	35.7	50.0	35.7	47.6	61.1	22.2	46.7
R	33.3	50.0	28.6	21.4	23.8	33.3	0.0	26.7
SC	33.3	35.7	42.9	21.4	**52.4**	61.1	**44.4**	46.7

Table 1 lists the overall and per class accuracy of each of the eight features using decision trees only due to the space limit owing to its improved and consistent performance. The table indicates that in general the thermal features extracted from the videos are better indicators of the degree of thermal discomfort. For the stage-wise experiments, the (avg) thermal feature

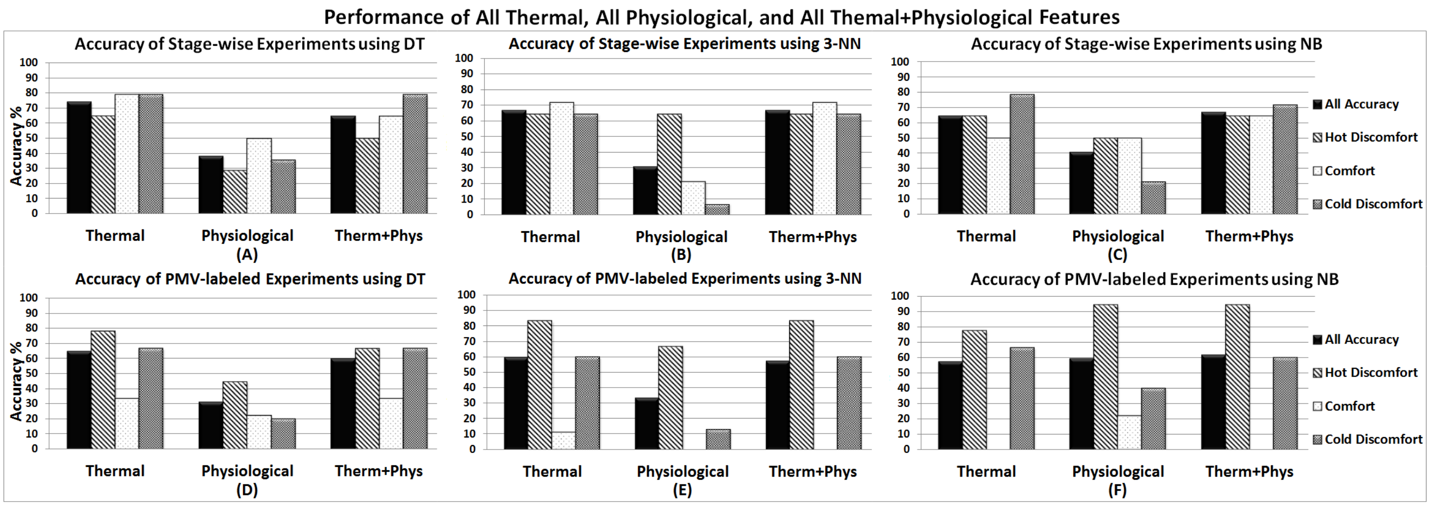

FIGURE 7. OVERALL AND PER CLASS ACCURACY PERCENTAGES USING ALL THERMAL FEATURES, ALL PHYSIOLOGICAL FEATURES, AND ALL 8 FEATURES COMBINED FOR STAGE-WISE EXPERIMENTS USING (A) DECISION TREES (DT), (B) K-NEAREST NEIGHBOR (3-NN), AND (C) NAIVE BAYES (NB), AND FOR PMV-LABELED EXPERIMENTS USING (D) DECISION TREES, (E) K-NEAREST NEIGHBOR, AND (F) NAIVE BAYES.

exhibits a significantly improved performance compared to other features. The improvement in the overall accuracy is approximately 28% compared to the second best performing feature (BVP) which has the best performance for the hot discomfort class. The performance of all features is better than the baseline except for the two physiological features, (R) and (SC).

The overall performance of the PMV-labeled experiments is lower than the stage-wise. The thermal feature (min) achieves the highest overall accuracy and the highest accuracy for the hot and cold discomfort classes. The physiological measurement (SC) also achieves the highest overall accuracy and the highest accuracy for the comfort class. The trend of the poor performance of the comfort class can be observed with all features here as well. In particular, four features have an accuracy that is below the base line and three features perform slightly better than the base line for the PMV-labeled experiments.

To further detect the thermal and physiological features combinations that have higher capability of discriminating between the three classes, Fig. 8 shows the overall and per class accuracy of the best combination of selected features using the Plus-L Take-Away-R method for the thermal features, physiological features, and all eight features for the stage-wise and PMV-labeled experiments. The selected features are shown in parentheses in the figure. The thermal selected features exhibit an improved performance once again compared to the selected physiological features except for Fig. 8 (F). However, on the contrary of training all eight features previously, selecting the best features out of the combination of the eight features increases the overall accuracy in all cases except Fig. 8 (C), where the best selected feature is the thermal (avg).

It can be noted that the (avg) thermal feature is repeatedly selected in most cases whether by itself or in combination with other features except for Fig. 8 (E). As with individual feature performances, this specific feature has high capability of differentiating between different levels of discomfort. Adding selected physiological features to the thermal (avg), further improves the performance such as adding the BVP and R features. For the PMV-labeled experiments, it can once again be noticed that the comfort class performance suffers especially with nearest neighbor and Naive Bayes classifiers while the performance of the hot discomfort class is improved.

Comfort Class Performance

Our analysis indicates that the comfort class suffers a deteriorated performance, especially with the PMV-labeled experiments. In order to investigate this issue, we decided to visualize the changes that occur from one stage to another. For visualization, the average thermal feature (avg), which averages the pixel values of the face area, is used because of its improved performance and capability of discriminating between classes.

Figure 9 illustrates the variation of the feature through the three experimental stages for all 14 occupants. The y-axis represents the values for the pixels averages, where higher pixel values represent higher temperatures. The x-axis represents the number of frames used for the 10 seconds per stage experiments. Each stage has 150 frames. The hot discomfort stage ranges from (1 to 150) frames, the comfort stage ranges from (151 to 300) frames, and the cold discomfort stage ranges from (301 to 450) frames. Surprisingly, the comfort stage curves clarifies that the average

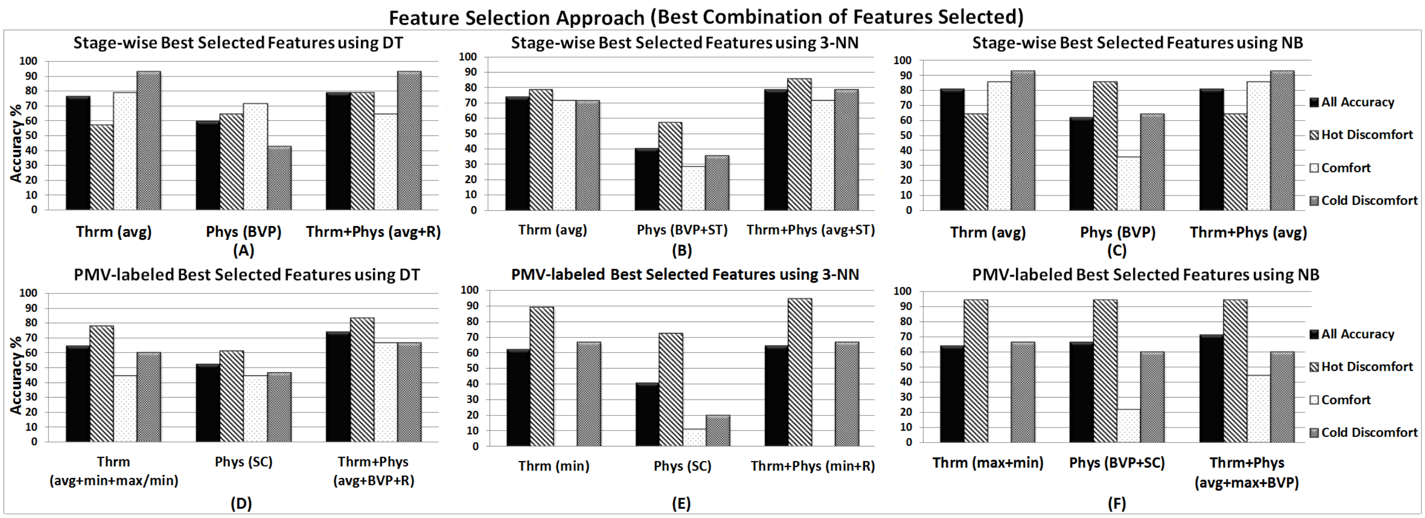

FIGURE 8. OVERALL AND PER CLASS ACCURACY USING FEATURE SELECTION FOR STAGE-WISE EXPERIMENTS USING (A) DECISION TREES (DT), (B) K-NEAREST NEIGHBOR (3-NN), AND (C) NAIVE BAYES (NB), AND FOR PMV-LABELED EXPERIMENTS USING (D) DECISION TREES, (E) K-NEAREST NEIGHBOR, AND (F) NAIVE BAYES. SELECTED FEATURES ARE SHOWN IN PARENTHESES.

pixel values are higher than the hot discomfort stage, i.e., the face cells have higher temperatures during this stage.

In hot weather, the blood flow transfers the heat from the body core to the skin where the heat is lost mainly by thermal convection and radiation and to a lesser degree by thermal conduction. Five minutes following the activity, we assumed that the occupants will start to go into a comfort state. However, the curves make it clear that the temperature is still increasing during this stage for each occupant due to the delay (inertia) of the heat transfer process (mainly natural convection and radiation). While the general trend shows a temperature increase in the comfort stage, some occupants have higher temperature in the hot discomfort stage compared to other occupants in the comfort stage. Moreover, the distribution of the classes using the PMV survey shows that more occupants were still thermally uncomfortable while only nine claimed they are thermally comfortable. On the other hand, the cold discomfort class (forced convection is used) shows a clear decrease in the temperature indicating that the body has adapted in a faster manner to cold discomfort.

The results of training the classifiers, especially with the PMV-labeled data, show that the classifiers could not discriminate between the hot discomfort and comfort classes. In multiple cases, the classifiers considered most thermally comfortable instances as hot discomfort, which was reflected in its improved performance. The peaks that are seen in the black curve shown in right-bottom side of Fig. 9 are for an occupant who had her/his hair covering the forehead down to the eyes. In some frames, the binarization process could not completely eliminate those hair areas and considered them part of the skin, which obviously influenced the calculation of the average of the pixel values.

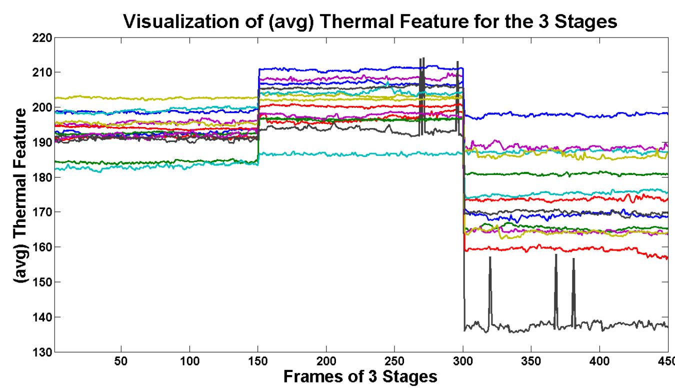

FIGURE 9. VARIATIONS IN THE THERMAL (AVG) FEATURE THROUGH THE THREE STAGES OF HOT DISCOMFORT, COMFORT, AND COLD DISCOMFORT/

CONCLUSION AND FUTURE WORK

Automated detection of thermal discomfort could play a significant role in designing energy-efficient buildings, which in turn would have beneficial consequences on the climate and environment. This paper contributes a novel dataset consisting of sensorial measurements of the human body and a multimodal model that automatically detects thermal discomfort based on thermal features and supported with physiological measurements obtained from an indoor environment.

Two sets of experimental data were acquired, first (i) from a three stage set that had an equal distribution of instances among three classes of hot discomfort, comfort, and cold discomfort, and (ii) PMV-labeled experiments with self-reported distribution of classes. The paper then presented two approaches to create a model that learns to discriminate between the three classes, namely the bag of visual words approach and feature selection approach. While the feature selection approach exhibited an improved performance compared to the bag of visual words, both approaches illustrated similar trends. For example, the stage-wise experiments performed better than the PMV-labeled experiments. Moreover, the comfort class exhibited a deteriorated performance, especially with the PMV-labeled experiments, compared to the detection of the hot and cold discomfort classes.

In general the thermal features achieved higher capability of detecting the occupants' level of comfort/discomfort compared to the physiological measurements. In particular, the average thermal pixel values indicated a superior capability of differentiating between different classes. However, selecting the combination of features that achieves the best performance showed that adding selected physiological measurements to the selected thermal features can slightly enhance the performance.

Further analysis indicated that the observed deteriorated performance of the comfort class is related to the fact that during the assumed state of thermal comfort (stage 2) most subjects did not cooled down sufficiently or were even "hotter" that in the first stage (activity on an elliptical machine). This is obviously due to the built in cooling mechanism of the human body and the inertia of the heat transfer processes involved. As a results the temperature of the body kept increasing for an extended amount of time, and hence it was classified as hot discomfort in many cases.

For future work, we are planning to collect additional data from more occupants to be able to generalize well to different states of discomfort. Although we have reached an overall accuracy of approximately 80% for our system in some cases, we expect additional important improvement after addressing some of the issues observed while carrying out this set of experiments. For instance, the poor comfort class performance can be addressed using one of two strategies. First, the sequence of the experimental stages can be altered so that we start with the comfort stage followed by the cold discomfort stage and then the activity to simulate the hot discomfort stage. In this case, the comfort class will not be affected by any previous states of discomfort. Second, the duration allowed for each stage can be increased from a total of 30 minutes to an hour, which would allow enough time for a subjects's body to adapt to the thermal conditions before moving into the next thermal state. The clothing level and relative humidity parameters will also be added at a later time.

The ultimate goal of this research is determining the features that are capable of detecting the state of discomfort and help set guidelines and create systems for energy conservation of buildings (minimize energy consumption) while maintaining thermal comfort of their inhabitants.

ACKNOWLEDGMENTS

We are grateful to Prof. Bill Buckles from the University of North Texas for allowing us to use the thermal camera. This material is based in part upon work supported by National Science Foundation award #1355633. Any opinions, findings, and conclusions or recommendations expressed in this material are those of the authors and do not necessarily reflect the views of the National Science Foundation.

REFERENCES

[1] , 2013. Residential energy consumption survey. Tech. rep., U.S. Energy Information Administration, May.

[2] Aebischer, B., Catenazzi, G., and Jakob, M., 2007. "Impact of climate change on thermal comfort, heating and cooling energy demand in europe". In Proceedings ECEEE 2007 Summer Study "Saving Energy Just Do It!", pp. 23–26.

[3] Mller, N., Kuttler, W., and Barlag, A.-B., 2014. "Counteracting urban climate change: adaptation measures and their effect on thermal comfort". *Theoretical and Applied Climatology,* ***115***(1-2), pp. 243–257.

[4] Leech, J., Burnett, R., Nelson, W., Aaron, S., and Raizenne, M., 2000. "Outdoor air pollution epidemiologic studies". *American Journal of Respiration and Critical Care Medicine,* ***161***(3).

[5] Hoppe, P., 2002. "Different aspects of assessing indoor and outdoor thermal comfort". *Energy and Buildings,* ***34***(4).

[6] , 1997. "Ashrae (american society of heating and refrigerating engineers)". In Handbook of Fundamentals: Physiological Principles, Comfort, Health.

[7] Mayer, E., 1993. "Objective criteria for thermal comfort". *Building and Environment,* ***28***(4), pp. 399 – 403.

[8] Fanger, P., 1972. *Thermal Comfort*. McGraw-Hill Book Company, New York, NY, USA.

[9] Hoppe, P. R., and Seidl, H. A., 1991. "Problems in the assessment of the bioclimate for vacationists at the seaside". *International Journal of Biometeorology,* ***35***(2), pp. 107–110.

[10] Rohles, F. H., 2007. "Temperature and temperament: A psychologist looks at comfort". *ASHRAE Transactions,* ***49***, pp. 14–19.

[11] Tredre, B. E., 1965. "Assessment of mean radiant temperature in indoor environments". *British Journal of Industrial Medicine,* ***22***(1), pp. 58–66.

[12] Arora, N., Martins, D., Ruggerio, D., Tousimis, E., Swistel, A. J., Osborne, M. P., and Simmons, R. M., 2008. "Effectiveness of a noninvasive digital infrared thermal imaging system in the detection of breast cancer". *The American Journal of Surgery,* ***196***(4), pp. 523 – 526.

[13] Ng, E.-K., 2009. "A review of thermography as promising non-invasive detection modality for breast tumor". *International Journal of Thermal Sciences,* ***48***(5), pp. 849 – 859.

[14] Garbey, M., Sun, N., Merla, A., and Pavlidis, I., 2007. "Contact-free measurement of cardiac pulse based on the analysis of thermal imagery". *IEEE Transactions on Biomedical Engineering,* ***54***(8), pp. 1418–1426.

[15] Gulyaev, Y. V., Markov, A. G., Koreneva, L. G., and Zakharov, P. V., 1995. "Dynamical infrared thermography in humans". *IEEE Engineering in Medicine and Biology Magazine,* ***14***(6), pp. 766–771.

[16] Fabrice De Oliveira, Sophie Moreau, C. G., and Dittmar, A., 2007. "Infrared imaging analysis for thermal comfort assessment". In 29th Annual International Conference of the IEEE Engineering in Medicine and Biology Society, pp. 3373–3376.

[17] Oliveira, F. D., and Moreau, S., 2009. "Assessment of thermal environment sensation for various climatic conditions and fluctuating air flow". In EACWE 5.

[18] Zeiler, W., Boxem, G., van Houten, R., Vissers, D., and Maaijen, R., 2012. "The human leading the thermal comfort control". In Twelfth International Conference for Enhanced Building Operations, pp. 23–26.

[19] Maia, A. P. d. A., Oliveira, S. R. d. M., Moura, D. J. d., Sarubbi, J., Vercellino, R. d. A., Medeiros, B. B. L., and Griska, P. R., 2013. "A decision-tree-based model for evaluating the thermal comfort of horses". *Scientia Agricola,* ***70***, 12, pp. 377 – 383.

[20] Freire, R. Z., Oliveira, G. H., and Mendes, N., 2008. "Predictive controllers for thermal comfort optimization and energy savings". *Energy and Buildings,* ***40***(7), pp. 1353 – 1365.

[21] Haldi, F., and Robinson, D., 2008. "On the behaviour and adaptation of office occupants". *Building and Environment,* ***43***(12), pp. 2163 – 2177.

[22] Huizenga, C., Abbaszadeh, S., Zagreus, L., and Arens, E. A., 2006. "Air quality and thermal comfort in office buildings: Results of a large indoor environmental quality survey". In Healthy Buildings, pp. 393–397.

[23] Fang, L., Wyon, D. P., Clausen, G., and Fanger, P. O., 2004. "Impact of indoor air temperature and humidity in an office on perceived air quality, sbs symptoms and performance". *Indoor Air,* ***14***, pp. 74–81.

[24] Zheng, G., Jing, Y., Huang, H., and Ma, P., 2009. "Thermal comfort and indoor air quality of task ambient air conditioning in modern office buildings". In Information Management, Innovation Management and Industrial Engineering, 2009 International Conference on, Vol. 2, pp. 533–536.

[25] Balaras, C. A., Dascalaki, E., and Gaglia, A., 2007. "HVAC and indoor thermal conditions in hospital operating rooms". *Energy and Buildings,* ***39***(4), pp. 454 – 470.

[26] Ye, X. J., Zhou, Z. P., Lian, Z. W., Liu, H. M., Li, C. Z., and Liu, Y. M., 2006. "Field study of a thermal environment and adaptive model in shanghai". *Indoor Air,* ***16***(4).

[27] Bessoudo, M., 2008. *Building Façades and Thermal Comfort: The Impacts of Climate, Solar Shading, and Glazing on the Indoor Thermal Environment*. VDM Publishing.

[28] Homod, R. Z., Sahari, K. S. M., Almurib, H. A., and Nagi, F. H., 2012. "{RLF} and {TS} fuzzy model identification of indoor thermal comfort based on pmv/ppd". *Building and Environment,* ***49***(0), pp. 141 – 153.

[29] Hamdy, M., Hasan, A., and Siren, K., 2011. "Impact of adaptive thermal comfort criteria on building energy use and cooling equipment size using a multi-objective optimization scheme". *Energy and Buildings,* ***43***(9).

[30] Stathopoulos, T., Wu, H., and Zacharias, J., 2004. "Outdoor human comfort in an urban climate". *Building and Environment,* ***39***(3), pp. 297 – 305.

[31] Zhang, Y., and He, J., 2012. "Measurement and analysis of thermal environment in a nanning's pedestrian street". In 2012 2nd International Conference on Consumer Electronics, Communications and Networks (CECNet).

[32] Ali-Toudert, F., and Mayer, H., 2007. "Thermal comfort in an eastwest oriented street canyon in freiburg (Germany) under hot summer conditions". *Theoretical and Applied Climatology,* ***87***(1-4), pp. 223–237.

[33] Ismail, A. R., Jusoh, N., Ibrahim, M. H., Panior, K. N., Zin2, M. Z. M., Hussain, M. A., and Makhtar3, N. K., 2010. "Thermal comfort assessment in computer lab: A case study at ungku omar polytechnic malaysia". In National Conference in Mechanical Engineering Research and Postgraduate Students, pp. 408–416.

[34] Karjalainen, S., 2007. "Gender differences in thermal comfort and use of thermostats in everyday thermal environments". *Building and Environment,* ***42***(4), pp. 1594–1603.

[35] Dang, C., Iwai, M., Umeda, K., Tobe, Y., and Sezaki, K., 2012. "Navicomf: Navigate pedestrians for comfort using multi-modal environmental sensors". In 2012 IEEE International Conference on Pervasive Computing and Communications (PerCom), pp. 76–84.

[36] Dang, C., Iwai, M., Tobe, Y., Umeda, K., and Sezaki, K., 2013. "A framework for pedestrian comfort navigation using multi-modal environmental sensors". *Pervasive and Mobile Computing,* ***9***(3), pp. 421 – 436.

[37] Ashrae, 2007. "Ashrae publishes residential air quality standard".

[38] Viola, P., and Jones, M., 2004. "Robust real-time face detection". *International Journal of Computer Vision,* ***57***(2), pp. 137–154.

[39] Sezgin, M., and Sankur, B., 2004. "Survey over image thresholding techniques and quantitative performance evaluation". *Journal of Electronic Imaging,* ***13***(1), pp. 146–168.

[40] Ferri, F. J., Pudil, P., Hatef, M., and Kittler, J., 1994. "Comparative study of techniques for large-scale feature selection". *Pattern Recognition in Practice IV (E. S. Gelsema and L. N. Kanal, eds.), Elsevier Science B.V.*, pp. 403–413.